# Effective pore-scale dispersion upscaling with a correlated continuous time random walk approach

Tanguy Le Borgne, Diego Bolster, Marco Dentz, Pietro de Anna, Alexandre Tartakovsky

# Effective pore-scale dispersion upscaling with a correlated continuous time random walk approach

T. Le Borgne,[1] D. Bolster,[2] M. Dentz,[3] P. de Anna,[1] and A. Tartakovsky[4]

Received 23 January 2011; revised 29 September 2011; accepted 22 October 2011; published 29 December 2011.

[1] We investigate the upscaling of dispersion from a pore-scale analysis of Lagrangian velocities. A key challenge in the upscaling procedure is to relate the temporal evolution of spreading to the pore-scale velocity field properties. We test the hypothesis that one can represent Lagrangian velocities at the pore scale as a Markov process in space. The resulting effective transport model is a continuous time random walk (CTRW) characterized by a correlated random time increment, here denoted as correlated CTRW. We consider a simplified sinusoidal wavy channel model as well as a more complex heterogeneous pore space. For both systems, the predictions of the correlated CTRW model, with parameters defined from the velocity field properties (both distribution and correlation), are found to be in good agreement with results from direct pore-scale simulations over preasymptotic and asymptotic times. In this framework, the nontrivial dependence of dispersion on the pore boundary fluctuations is shown to be related to the competition between distribution and correlation effects. In particular, explicit inclusion of spatial velocity correlation in the effective CTRW model is found to be important to represent incomplete mixing in the pore throats.

**Citation:** Le Borgne, T., D. Bolster, M. Dentz, P. de Anna, and A. Tartakovsky (2011), Effective pore-scale dispersion upscaling with a correlated continuous time random walk approach, *Water Resour. Res.*, *47*, W12538, doi:10.1029/2011WR010457.

## 1. Introduction

[2] The ability to upscale dispersion is an important step in predicting solute transport through porous media. This topic has received continuous attention since the pioneering work of Taylor, who studied dispersion in a tube [*Taylor*, 1953]. Taylor showed that this system, at late times, once transverse diffusion has allowed the plume to sample all the velocities in the tube cross section, can be characterized by an effective one-dimensional advection-dispersion equation with an enhanced dispersion coefficient. This enhanced dispersion coefficient can be quantified by the second centered moment of the concentration distribution [*Aris*, 1956]. The Taylor dispersion coefficient reflects the interaction between spreading driven by the heterogeneous velocity field and diffusion that attenuates the resulting concentration contrasts.

[3] Since this seminal study there has been a large amount of work dedicated to quantifying dispersion in more complex flow fields. A variety of methodologies, including the method of local moments [*Brenner*, 1980; *Brenner and Adler*, 1982; *Frankel and Brenner*, 1989; *Edwards and Brenner*, 1993], volume averaging [*Bear*, 1972; *Plumb and Whitaker*, 1988; *Valdes-Parada et al.*, 2009; *Wood*, 2009], and the method of multiple scales [*Auriault and Adler*, 1995; *Lunati et al.*, 2002; *Attinger et al.*, 2001], have emerged. The main goal of these methods is to develop an effective asymptotic dispersion coefficient that quantifies spreading and mixing in an upscaled effective equation and in many cases they have been successful [*Edwards et al.*, 1991; *Porter et al.*, 2010].

[4] Macrodispersion approaches describe asymptotic heterogeneity-induced transport, which can be cast in an advection-dispersion equation for the macroscale solute concentration. Such Fickian models are characterized typically by a diffusive growth of the plume size. In many applications, however, such an asymptotic regime is often not reached on realistic space and time scales. In fact, there is a large amount of data from field [*Rehfeldt et al.*, 1992; *Gelhar et al.*, 1992; *Sidle et al.*, 1998; *Le Borgne and Gouze*, 2008] and laboratory experiments [*Silliman and Simpson*, 1987; *Silliman et al.*, 1987; *Moroni et al.*, 2007; *Levy and Berkowitz*, 2003] that suggests that the Fickian behavior is often not observed. Theoretical predictions in heterogeneous velocity fields anticipated this [*Matheron and de Marsily*, 1980; *Deng et al.*, 1993; *Deng and Cushman*, 1995; *Dentz et al.*, 2000; *Berkowitz et al.*, 2006; *Bijeljic and Blunt*, 2006; *Nicolaides et al.*, 2010; *Wood*, 2009]. This behavior can be traced back to incomplete mixing on the macroscopic support scale [*Le Borgne et al.*, 2011; *Dentz et al.*, 2011].

[5] Thus, for the realistic modeling of transport in heterogeneous porous media, it is necessary to predict transport

[1]Geosciences Rennes, UMR 6118, CNRS, Université de Rennes 1, Rennes, France.
[2]Environmental Fluid Dynamics Laboratories, Department of Civil Engineering and Geological Sciences, University of Notre Dame, Notre Dame, Indiana, USA.
[3]Institute of Environmental Assessment and Water Research, Barcelona, Spain.
[4]Computational Mathematics Group, Pacific Northwest National Laboratory, Richland, Washington, USA.


0043-1397/11/2011WR010457

during this preasymptotic regime [e.g., *Gill and Sankarasubramanian*, 1970; *Latini and Bernoff*, 2001; *Bijeljic and Blunt*, 2006] and in particular capture the anomalous non-Fickian behavior. Several nonlocal models have emerged to model this behavior in porous media, including moment equation approaches [*Neuman*, 1993; *Morales-Casique et al.*, 2006], projector formalisms [*Cushman and Ginn*, 1993, 1994], multirate mass transfer [*Haggerty and Gorelick*, 1995; *Carrera et al.*, 1998; *Cherblanc et al.*, 2007; *Chastanet and Wood*, 2008], fractional advection-dispersion equations [*Benson et al.*, 2000, 2001; *Cushman and Ginn*, 2000], continuous time random walks [*Berkowitz and Scher*, 1995; *Berkowitz et al.*, 2006; *Bijeljic and Blunt*, 2006] and continuous Markovian stochastic processes in time [*Meyer and Tchelepi*, 2010]. A review of these models is provided by *Neuman and Tartakovsky* [2009]. One of the main challenges within nonlocal modeling approaches is how to relate microscale properties (e.g., velocity statistics) to the effective macroscale models.

[6] In this paper we will focus on the continuous time random walk (CTRW) approach. A popular approach for defining CTRW model parameters is breakthrough curves fitting [e.g., *Berkowitz and Scher*, 2010]. While useful in practice, the limitation of this approach is that it is difficult in general to relate the derived effective parameters to the velocity field properties. Some analytical approaches considering simplified forms of heterogeneity have been developed that upscale exactly to a CTRW [*Dentz and Castro*, 2009; *Dentz et al.*, 2009; *Dentz and Bolster*, 2011]. In particular, the importance of spatial velocity correlation and its impact on anomalous transport is explicitly illustrated in the simplified model of *Dentz and Bolster* [2011]. A different approach that is not restricted to simplified types of heterogeneity was developed by *Le Borgne et al.* [2008a, 2008b]. By using the spatial Markov property of Lagrangian velocities, one can define a correlated CTRW model, whose parameters are defined from the velocity field distribution and spatial correlation properties. Thus, the upscaled CTRW model is obtained without fitting its parameters to the dispersion data; instead they are estimated from the Lagrangian velocity field analysis. Velocity distribution and spatial correlation are known two govern dispersion heterogeneous media [*Bouchaud and Georges*, 1990]. Solute dispersion is enhanced when the width of the velocity distribution is increased. It is also enhanced when the spatial correlation of the velocity field is stronger. In other words, when each solute particle tends to keep similar velocities for a long time, the ensemble of particles is more dispersed. The correlated CTRW approach quantifies separately distribution and correlation effects. We will show in the following that this is critical to understand and quantify pore-scale dispersion as velocity distribution and spatial correlation can have antagonist effects, hence competing for governing the global dispersion.

[7] Here we invoke a CTRW approach characterized by correlated successive particle velocities (termed correlated CTRW in the following) to study dispersion in a pore-scale context. To this end, we first consider a simplified periodic representation of a pore introduced by *Dykaar and Kitanidis* [1996] (Figure 1) and then a more complex two-dimensional heterogeneous porous medium [*Tartakovsky and Neuman*, 2008]. Because of its simplicity, the sinusoidal channel model can provide much insight to the understanding of basic mechanisms that occur at the pore scale. The conclusions derived from the analysis of this system can also be used to understand and quantify the role of boundary fluctuations, which is relevant for example for transport at the fracture scale [*Drazer et al.*, 2004; *Drazer and Koplick*, 2002]. Additionally this model is appealing, because, while quite simple, it displays some interesting and perhaps unexpected features. For example, *Bolster et al.* [2009] showed that increasing the fluctuation of the pore wall does not necessarily result in an increase in asymptotic dispersion, a result that may be counterintuitive on the basis of other predictions [e.g., *Gelhar*, 1993; *Prude'Homme and Hoagland*, 1999; *Tartakovsky and Xiu*, 2006] that suggest that as the fluctuations increase, so too should dispersion. Some experimental evidence [*Drazer et al.*, 2004; *Drazer and Koplick*, 2002] and heuristic mathematical arguments [*Rosencrans*, 1997] support this prediction of a reduction in asymptotic dispersion. The reduction cannot be explained by a classical Taylor-Aris type approach (see *Bolster et al.* [2009] for details).

[8] In this work, we argue and illustrate that the correlated CTRW model provides a solid framework that can be used to physically interpret and understand such observations. Additionally we illustrate that it is capable of accurately predicting the evolution of observed preasymptotic non-Fickian dispersion. In section 2, we describe the periodic pore representation for which we seek to upscale dispersion. In section 3, we introduce the correlated CTRW model and compute the transition time distribution and the probability transition matrix that parametrize it. In section 4, we compare the prediction of this upscaled model to the results obtained from the fully resolved pore-scale simulations. In section 5, we demonstrate the applicability of this upscaling approach to a more complex heterogeneous porous medium.

## 2. Sinusoidal Channel Model

[9] We consider flow in a two-dimensional channel that is symmetric about the central axis at $y = 0$. The boundaries of the channel fluctuate periodically in the horizontal direction as

$$h(x) = \overline{h} + h' \sin\left(2\pi \frac{x}{L}\right), \tag{1}$$

where $\overline{h}$ is the average channel height. The aspect ratio is defined by

$$\epsilon = \frac{2\overline{h}}{L}. \tag{2}$$

The ratio between the amplitude of the aperture fluctuations $h'$ and the mean aperture, called the fluctuation ratio, is denoted by

$$a = \frac{h'}{2\overline{h}}. \tag{3}$$

The flow at low Reynolds numbers within such a sinusoidal channel, whose boundary changes slowly (i.e., $\epsilon = \frac{\overline{h}}{L} < 1$) was studied and derived analytically using a perturbation method in $\epsilon$ by *Kitanidis and Dykaar* [1997]. In order to

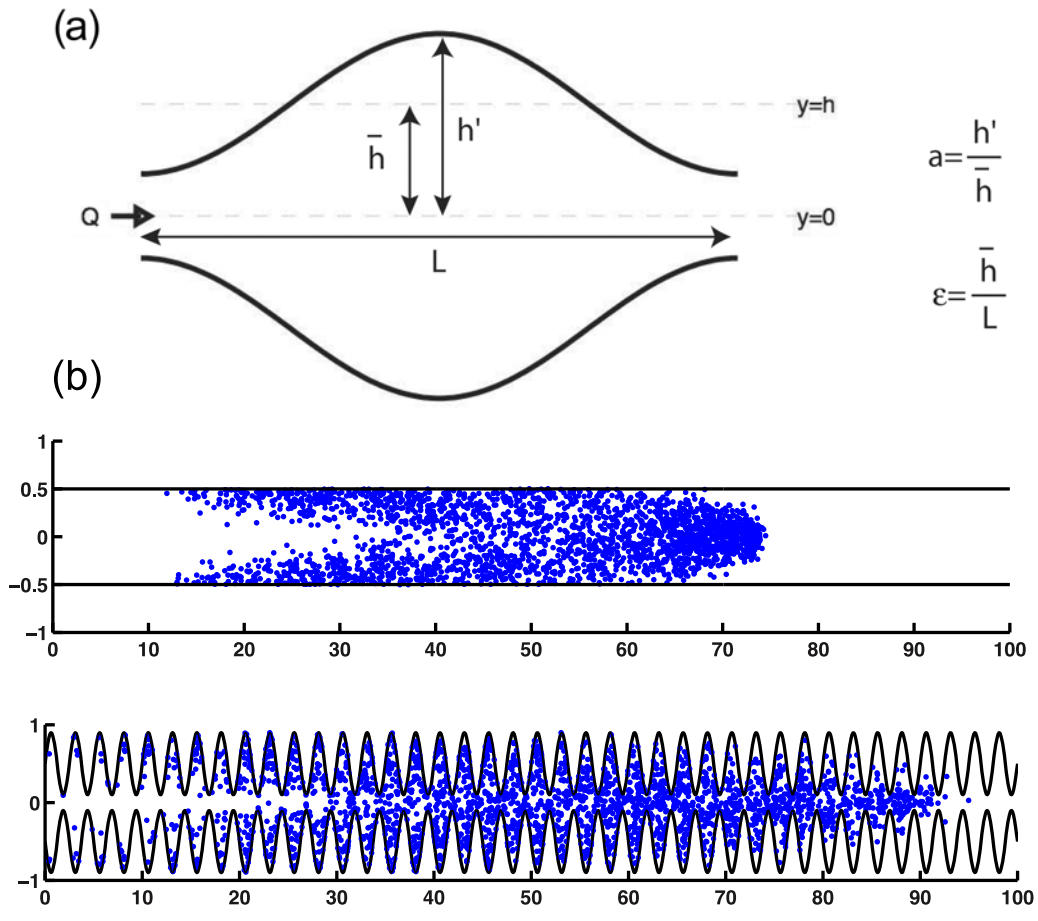


**Figure 1.** (a) A schematic of the pore we are considering and (b) random walk simulations for $Pe = 10^3$ after a time of $50\tau$ (where $\tau$ is the mean travel time of one pore). In Figure 1b, the top plot corresponds to $a = 0$, and the bottom plot corresponds to $a = 0.4$ and $\epsilon = 0.4$.

illustrate the different types of flow that can arise within such a geometry, two sets of streamlines calculated using this method are shown in Figure 1. A feature of this model is that recirculation zones appear for aspect and fluctuation ratios close to 0.4 [*Bolster et al.*, 2009].

[10] We simulate transport in this flow field using a particle tracking approach. The Peclet number $Pe$, which characterizes the ratio between the advective and diffusive time scales, is defined by

$$Pe = \frac{2\bar{h}\bar{u}}{D}, \tag{4}$$

where $D$ is the diffusion coefficient and $\bar{u}$ is the mean velocity. In the following simulations, we set the parameter values as $Pe = 10^3$, $\bar{u} = 1$, and $\bar{h} = 1/2$. Figure 2 shows an example of particle trajectories in a flow field characterized by $a = 0.4$ and $\epsilon = 0.4$. Particles travel fast at the center of the pore and move slowly close to the pore wall where they can be trapped in recirculation zones. They jump from one streamline to another by diffusion. The resulting longitudinal dispersion can be characterized in terms of the longitudinal width $\sigma$ of the solute distribution $c(\mathbf{x}, t)$

$$\sigma^2(t) = \int d\mathbf{x} x^2 c(\mathbf{x}, t) - \left[\int d\mathbf{x} x c(\mathbf{x}, t)\right]^2. \tag{5}$$

Specifically, asymptotic longitudinal dispersion is quantified in terms of the effective dispersion coefficient

$$D^e = \frac{1}{2}\lim_{t\to\infty} \frac{d\sigma^2(t)}{dt}. \tag{6}$$

[11] The dependence of the asymptotic coefficient on the aspect and fluctuation ratios, obtained by *Bolster et al.* [2009], is displayed in Figure 3. When the aspect ratio $\epsilon$ is small, the increase of the fluctuation ratio $a$ leads to a decrease of the asymptotic dispersion coefficient. On the other hand, when the aspect ratio $\epsilon$ is large, the increase of the fluctuation ratio $a$ leads to an increase of the asymptotic dispersion coefficient. We demonstrate in the following that this nontrivial behavior can be understood qualitatively by the competition between distribution effects and correlation effects and can be quantified formally through a correlated CTRW model.

## 3. Correlated CTRW Model

[12] We seek to represent the longitudinal dispersion process in the wavy channel model as a one-dimensional random walk with distributed spatial and temporal increments (CTRW). The series of successive longitudinal particle positions $\{x^{(n)}\}_{n=0}^{\infty}$ and travel times $\{t^{(n)}\}_{n=0}^{\infty}$ are

$$x^{(n+1)} = x^{(n)} + \Delta x^{(n)} \tag{7}$$

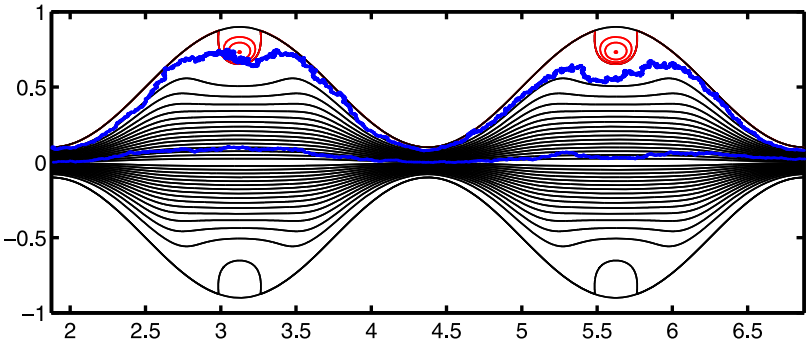


**Figure 2.** Examples of particle trajectories over two pores for two particles starting initially close to the pore wall and at the center of the pore throat, respectively. The pore shape parameters are $\epsilon = 0.4$ and $a = 0.4$. The detailed streamlines in the upper recirculation zones are shown in red.

$$t^{(n+1)} = t^{(n)} + \Delta t^{(n)}, \tag{8}$$

where $\{\Delta x^{(n)}\}_{n=0}^{\infty}$ and $\{\Delta t^{(n)}\}_{n=0}^{\infty}$ are the successive spatial and temporal increments. In many CTRW models, the successive temporal increments $\Delta t^{(n)}$ are taken as independent random variables. Thus, the dispersion dynamics depend entirely on the increment distributions [*Berkowitz and Scher*, 2010; *Dentz and Bolster*, 2011]. Figure 2 suggests that, in the absence of complete mixing at pore throats, there can be a significant correlation between successive particle travel times. Particles moving quickly at the pore center have a high probability to remain in a high-velocity zone in the next pore. Similarly, particles have a significant probability to be successively trapped in successive pores when they travel close to the pore walls.

[13] Transit times are related to Lagrangian velocities by $\{\Delta t^{(n)} = \Delta x / v^{(n)}\}_{n=0}^{\infty}$, where $v^{(n)}$ is the mean particle velocity across the length $\Delta x$. Diffusive jumps of particles across streamlines induce a certain velocity decorrelation such that ultimately the velocity memory is lost when the particle has traveled over many pores. The process of velocity decorrelation by diffusion is most efficient at the pore throat where streamlines converge close to each other. Figure 4 displays the pore-scale Lagrangian velocity correlation functions as a function of travel time and as a function of travel distance for the case $a = 0.4$ and $\epsilon = 0.4$. The Lagrangian velocities are found to have a short-range correlation in space and a long-range correlation in time. The latter is related to the low-velocity areas close to the pore wall and to the recirculation areas, where particles can remain trapped for a long time.

[14] In order to quantify the correlation between successive temporal increments, due to incomplete mixing at pore throats, we represent the series of successive transit times over one pore length $\{\Delta t^{(n)}\}_{n=0}^{\infty}$ as a Markov chain, which is motivated by the short range spatial correlation of Lagrangian velocities (Figure 4). Note that this the Markov property does not mean that the correlation length is assumed to be equal to one pore size. The corresponding correlation length depends on the transition probabilities for successive transit times. Thus, setting the spatial increment equal to the pore length $\Delta x^{(n)} = L$ in (7), the corresponding effective transport model is a correlated CTRW defined by the probability distribution density $p(\Delta t)$ and the conditional probability density $r(\Delta t|\Delta t')$, where $\Delta t$

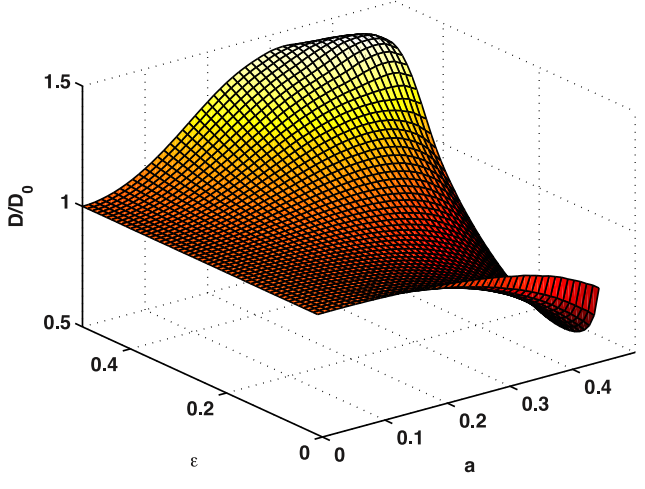


**Figure 3.** Dependence of the asymptotic dispersion coefficient on $\epsilon$ and $a$ for $Pe = 10^3$, from *Bolster et al.* [2009]. The dispersion coefficient is normalized by $D_0$, the value corresponding to a parallel wall channel ($\epsilon = 0$, $a = 0$).

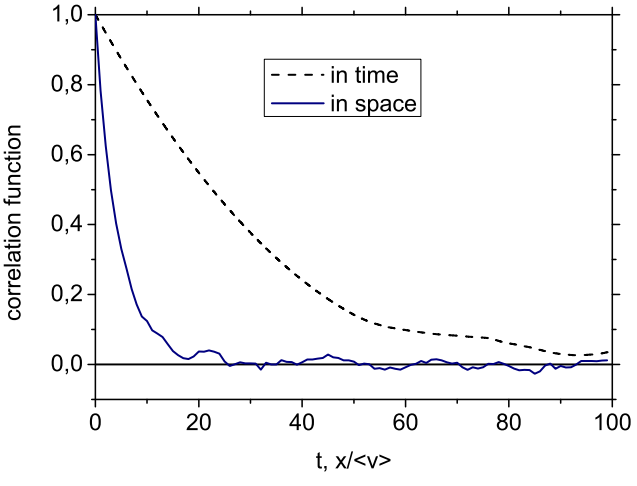


**Figure 4.** Comparison of pore-scale Lagrangian velocity correlation function in time and in space for parameters $a = 0.4$ and $\epsilon = 0.4$.

and $\Delta t'$ are successive transit times across one pore. To test the applicability of this model to upscale longitudinal dispersion, we numerically compute the transit time distributions across one pore $p(\Delta t)$ and the conditional probability density $r(\Delta t|\Delta t')$ from transport simulations over two pores (Figure 2).

[15] The Lagrangian transit time distributions across one pore $p(\Delta t)$, computed from particle tracking simulations, are displayed in Figure 5 for different values of the aspect and fluctuation ratios. They are characterized by a peak at small times and a tail at large times, with a significant probability for particles to experience large transit times. The maximum transit time is defined by an upper cut off. Both the minimum and maximum times depend on the pore shape. A special case is $a = 0.4$ and $\epsilon = 0.4$ for which recirculation zones exist (Figure 1c). The impact of these recirculation zones is that the width of the transit time distribution increases by about 1 order of magnitude compared to cases without recirculation zones. The probability of large transit times increases because of trapping of particles in these recirculation zones. At the same time, the smallest transit time decreases, i.e., the maximum velocity increases. This is due to an enhanced focusing of flow lines in the center of the pore (Figure 1c). For the other cases, the increase of the aspect ratio $\epsilon$ tends to slightly decrease the minimum transit time while increasing slightly the maximum transit time. The increase of the fluctuation ratio $a$ does not appear to affect the minimum transit time, but does increase slightly the maximum transit time.

[16] We now quantify the conditional probability density $r(\Delta t|\Delta t')$ from particle tracking simulations over two successive pores, where $\Delta t'$ is the transit time across the first pore and $\Delta t$ is the transit time across the second pore. This quantifies the correlation between successive transit time, illustrated in Figure 2. For this purpose, we discretize the transit time distribution $p(\Delta t)$ into $n$ classes $\{C_i\}_{1\le i\le n-1}$ of equal probability of occurrence [*Le Borgne et al.*, 2008b]. We define $\eta = P(\Delta t)$ as the score corresponding to the transit time $\Delta t$, where $P(\Delta t)$ is the cumulative transit time

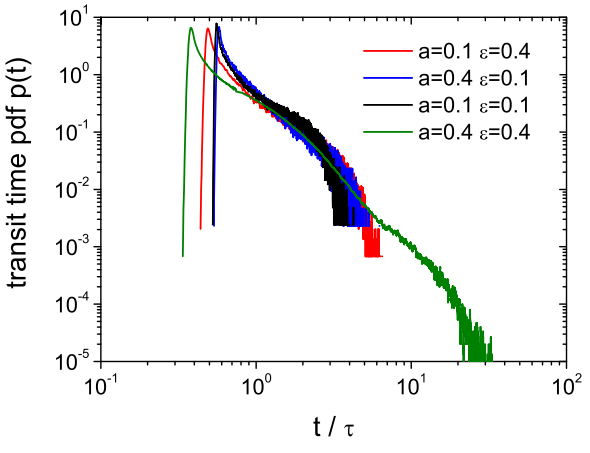


**Figure 5.** Transit time probability density function $p(t)$ across one pore corresponding to different values of the pore shape parameters $\epsilon$ and $a$. The transit time is normalized by the mean transit time over one pore $\tau$.

distribution. We discretize the $\eta$ domain, which is bounded between 0 and 1, into $n$ classes of equal width $1/n$, defined by their boundaries $\eta_i$. The smallest transit time (largest velocity) corresponds to $\eta_1 = 0$ and the largest transit time (smallest velocity) to $\eta_{n+1} = 1$. In this study, we use $n = 49$ classes. The influence of the number of classes on the prediction of spreading is discussed in section 4. For a given transit time $\Delta t$, the corresponding class $C_i$ is determined as follows: $\Delta t \in C_i$ if $\eta_i \le P(\Delta t) < \eta_{i+1}$. The corresponding class boundaries in the temporal increment space are $\Delta t_i = P^{-1}(\eta_i)$.

[17] The probability for a particle to travel through a pore in a time $\Delta t \in C_i$ given that it traveled through the previous pore in a time $\Delta t' \in C_j$ is given by,

$$T_{ij} = \int_{\Delta t_i}^{\Delta t_{i+1}} \mathrm{d}t \int_{\Delta t_j}^{\Delta t_{j+1}} \mathrm{d}t' r(t|t'), \tag{9}$$

The transition matrix $\mathbf{T}$ is the discrete form of the conditional probability density $r(\Delta t|\Delta t')$ and describes the transition probability from class $i$ to class $j$. The transition matrix is shown for different pore shapes in Figure 6. The transition probabilities are largest in the diagonal region and tend to zero away from the diagonal. The probabilities on the diagonal, i.e., $T_{ii}$, are the probabilities for a particle to remain in the same class $C_i$, i.e., to keep a similar transit time over successive pores. The probabilities away from the diagonal correspond to probabilities for a particle to change its transit time from one pore to another, which depends on its diffusion across streamlines.

[18] The correlation of successive times can be measured by the probability to remain in the original class and by the width of the banded matrix area around the diagonal, which reflects the probability for particles to remain in neighboring transit time classes over successive pores. Notice that the transition matrix quantifies some complex correlation properties of the flow field. For instance, the correlation is systematically stronger for small transit times (i.e., large velocities) than for large transit times (Figure 6). As shown in Figure 6, conditional probabilities in the upper left corner, corresponding to the probabilities for particles to keep small transit times, are higher than the other conditional probabilities, e.g., the probability for particles to keep intermediate or large transit times across successive pores.

[19] The comparison of transition matrices in Figure 6 can be used to understand the effect of the pore shape parameters (equation (2) and Figure 1a) on the transit time correlation. The effect of increasing the aspect ratio $\epsilon$ from 0.1 to 0.4 is to decrease the width of the banded area in the transition matrix around the diagonal, i.e., to increase the correlation of the successive transit times, as successive particle transit times have a high probability to be close to each other. This can be explained as follows. For a given mean channel height $\bar{h}$, increasing $\epsilon$ is equivalent to decreasing the pore length $L$. Decreasing $L$ implies decreasing the distance available for particles to diffuse across streamlines. Thus, for large $\epsilon$ the correlation of successive transit times is strong.

[20] For a given aspect ratio $\epsilon$, the effect of increasing the fluctuation ratio $a$ from 0.1 to 0.4 is to decrease the

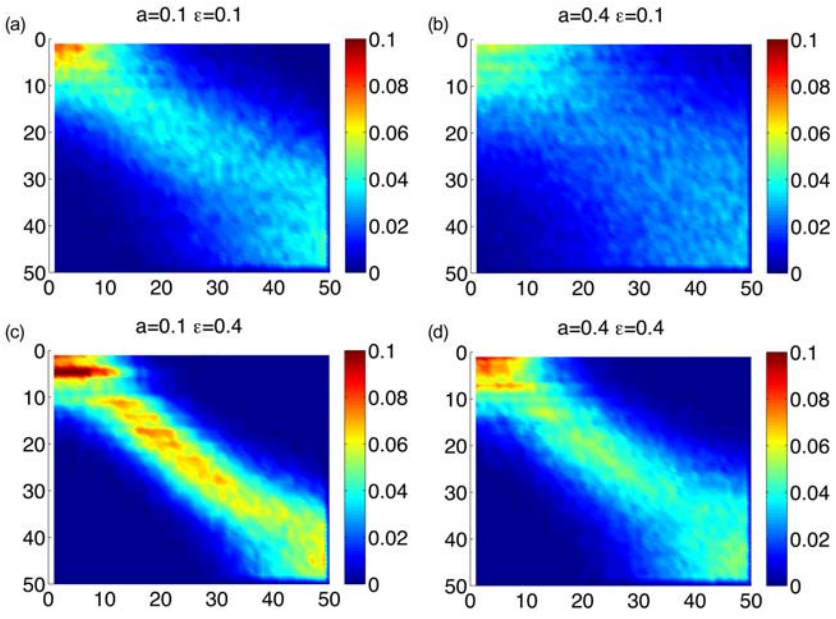


**Figure 6.** Spatial transition matrices $T$ corresponding to different values of the pore shape parameters $\epsilon$ and $a$ (equation (9)). The horizontal axis represents the initial transit time class and the vertical axis represents the next transit time class. Small matrix indices correspond to small transit times (large Lagrangian velocities), and large matrix indices correspond to large transit times (small Lagrangian velocities). The color scale represents the transit time transition probabilities along particle paths.

correlation of successive transit times, as shown by the increase of the width of the banded area in the transition matrix which implies that particle have a significant probability to change transit times over successive pores. This in turn can be explained by the small width of the pore necks for large $a$ (Figure 1a) that induces a focusing of flow lines, thus enhancing mixing between stream lines at the pore necks. Thus, for large $a$, the correlation between successive transit times is weak.

[21] The transit time distributions and correlation matrices can be used to understand the nontrivial dependence of the asymptotic dispersion coefficient on the pore shape parameters shown in Figure 3. In general, an increase in the width of transit time distribution and an increase of the correlation of successive transit times are both expected to contribute to an increase of the asymptotic dispersion coefficient. These effects are known as distribution- and correlation-induced dispersion [*Bouchaud and Georges*, 1990; *Dentz and Bolster*, 2011]. When changing the fluctuation ratio $a$, these two effects evolve in opposite directions, thus competing for controlling dispersion. An increase of the fluctuation ratio $a$ produces an increase the transit time variability but a decrease of there correlation over successive pores. In the absence of recirculation zones ($\epsilon < 0.4$), the transit time variability depends only slightly on the fluctuation ratio $a$. Since transit time decorrelation is the dominant effect in this case, the increase of the fluctuation ratio $a$ leads to a decrease of the asymptotic dispersion coefficient. Conversely, for large aspect ratios ($\epsilon \geq 0.4$), the appearance of recirculation zones leads to a strong dependence of the transit time distribution on the fluctuation ratio $a$. This effect dominates over the effect of transit time decorrelation, which implies that the asymptotic dispersion coefficient increases with the fluctuation ratio $a$ in this case. Thus, the dependence of dispersion coefficient on the pore shape parameters is controlled here by the competition between distribution and correlation effects.

## 4. Predictions of the Correlated CTRW Model

[22] The transit time distribution $p(\Delta t)$ and the transition matrix $\mathbf{T}$ together with the spatial Markov property define the correlated CTRW model in (8). Using this effective description, we can make predictions of the transport behavior over a large range of temporal and spatial scales. The equations of motion (8) of a particle are solved numerically using random walk particle tracking, which allows for efficient transport simulations. We compare the predictions of this effective random walk model with the numerical random walk simulations of transport through the fully resolved two-dimensional velocity fields (Figure 2) for $a = 0.4$ and $\epsilon = 0.4$. To probe the role of correlation we also compare the transport behavior resulting from the correlated CTRW with the predictions of a CTRW model without correlation, defined by (7) and (8) with the transition probability given as $r(\Delta t|\Delta t') = p(\Delta t)$. Notice that the predictions of both models are obtained without fitting the model parameters to the dispersion data. Instead the model's parameters, here $p(\Delta t)$ and $r(\Delta t|\Delta t')$ are estimated from the Lagrangian velocity field analysis.

[23] Figure 7 displays the temporal evolution of the second centered moment of the particle positions in the direction of the mean flow $\sigma^2(t)$ for the case $a = 0.4$ and $\epsilon = 0.4$. The initial preasymptotic regime, where $\sigma^2(t)$ evolves nonlinearly in time, lasts for about $30\tau$, where $\tau$ is the mean transit time across one pore. Hence, the Fickian behavior is reached when the average position of the plume has traveled over 30 pores. The spatial distribution of

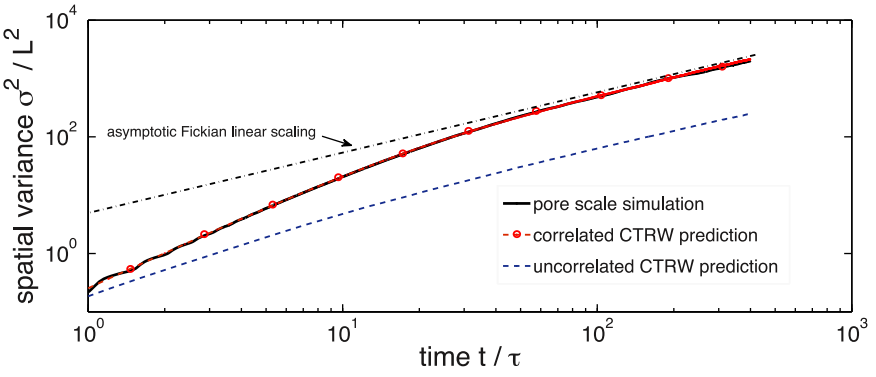


**Figure 7.** Comparison of the prediction of the correlated CTRW (red dashed line) and uncorrelated CTRW (blue dashed line) with the numerical simulations for the second centered spatial moment in the longitudinal direction $\sigma^2$, with $a = 0.4$ and $\epsilon = 0.4$ (black dots). The time is normalized by the mean transit time over one pore $\tau$, and the spatial variance is normalized by $L^2$. Notice the overlap of the correlated CTRW model predictions and the full pore-scale simulations.

particle positions, shown in Figure 8, is strongly non-Gaussian during the preasymptotic regime.

[24] The correlated CTRW model is found to provide very good predictions of the temporal evolution of the second centered moment $\sigma^2(t)$ at all times and is able to predict accurately the evolution of the spatial particle position distributions from non-Gaussian to Gaussian. In particular, the persistent asymmetry of the spatial distributions, which is due to trapping in low-velocity and recirculation zones, is well captured. The uncorrelated CTRW model is found to underestimate dispersion significantly. The discrepancy for the second centered moment $\sigma^2(t)$ is about 1 order of magnitude at large times. The uncorrelated CTRW model used here has the same transit time distribution as the correlated CTRW model but no correlation of successive transit times. Thus, the comparison of these two models shows the role of spatial correlations of particle motions, which are due in this example to incomplete mixing at the pore throats. Thus, successive transit time correlation, related for instance the fact that particles traveling close to the pore walls have a high probability of being successively trapped in recirculation zones (Figure 2), is found to have an important impact on dispersion.

[25] The good agreement of the correlated CTRW model with pore-scale simulations validates the spatial Markov property of Lagrangian velocities. This property implies that large-scale dispersion can be predicted from solving transport in just two characteristic pore sizes. The model parameters are fully defined from the Lagrangian velocity properties. We have performed the same comparison for a variety of other pore shape parameters and found a similar agreement between effective and pore-scale random walk simulations. The transition matrices quantify high-order correlation effects that are not included in classical two-point correlation functions. The high probability region in the left upper part of the transition matrices (Figure 6) indicate that small transit times are more correlated than large transit times. This implies that large velocities at the center of the pore are more correlated over successive pores than small velocities. The dependency of correlation on the local velocity was previously demonstrated by *Le Borgne et al.* [2007].

[26] In order to probe the minimum number of parameters sufficient to capture this effect, we ran correlated CTRW simulations with different numbers of transit time classes (Figure 9). Decreasing the number of classes from 49 to 12 we found only a slight change in the prediction of spatial variance. However, for a smaller number of classes, the spatial variance is significantly underestimated. For instance, the underestimation is about 40 percent when using only 3 velocity classes. Thus, we estimate that the minimum number of classes required in this case for capturing the whole range of correlation effects may be around 10. This suggests that, although the transition matrix can be simplified, it should contain a minimum of information for representing complex correlation properties such as the dependency of correlation on velocity.

## 5. Application to a Heterogeneous Porous Medium

[27] In section 5, we apply the methodology to the more complex 2-D heterogeneous porous medium studied by *Tartakovsky and Neuman* [2008] and *Tartakovsky et al.* [2008]. The Navier-Stokes equations for flow in the pore network are solved using smoothed particle hydrodynamics

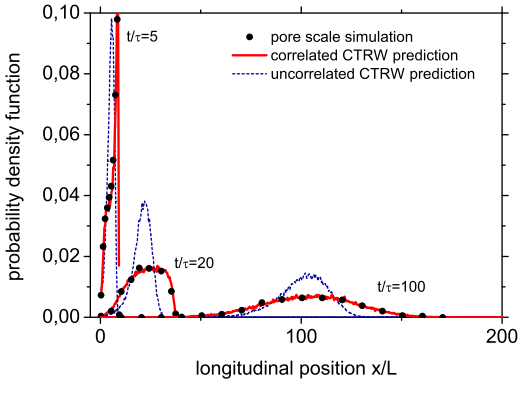


**Figure 8.** Comparison of the prediction of the correlated CTRW (red lines) and uncorrelated CTRW (blue lines) with the numerical simulations for the spatial distribution of longitudinal particle positions (black line with dots). Notice the overlap of the correlated CTRW model predictions and the full pore-scale simulations.

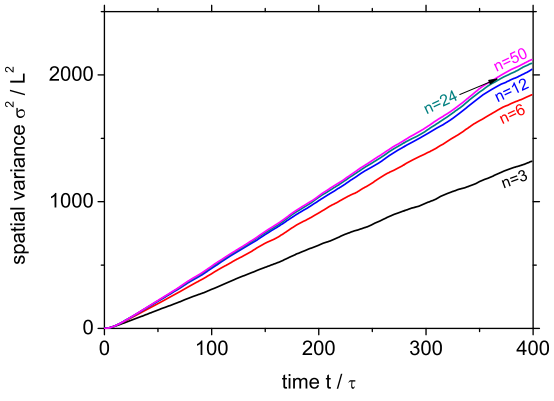


**Figure 9.** Prediction of the correlated CTRW model for the second centered moment with different numbers of velocity classes, $n = 3, 6, 12, 24, 49$.

(SPH) (Figure 10). The medium is composed of void and circular grains with mean porosity $\phi = 0.42$. The average velocity of $\overline{v} = 10^{-2}$ results from application of a hydraulic head gradient from top to bottom. The boundary conditions for flux are periodic on all sides. All details of computations are given by *Tartakovsky and Neuman* [2008]. The resulting velocity field shows the existence of a braided network of preferential flow paths as well as low-velocity or stagnation zones.

[28] In order to quantify the dispersion process in this medium, we apply the methodology to analyze the statistics of transit times along the SPH particle trajectories. SPH is a Lagrangian particle method where particles representing elementary fluid volumes are advected with the flow and exchange mass between them by diffusion. Advective Lagrangian trajectories are thus given by the trajectories of the SPH particles. The Lagrangian velocities analyzed along SPH particles trajectories can change because of advective heterogeneities but not because of diffusion across streamlines. Hence, velocity decorrelation occurs solely because of randomness in the velocity resulting from the heterogeneous nature of the porous medium.

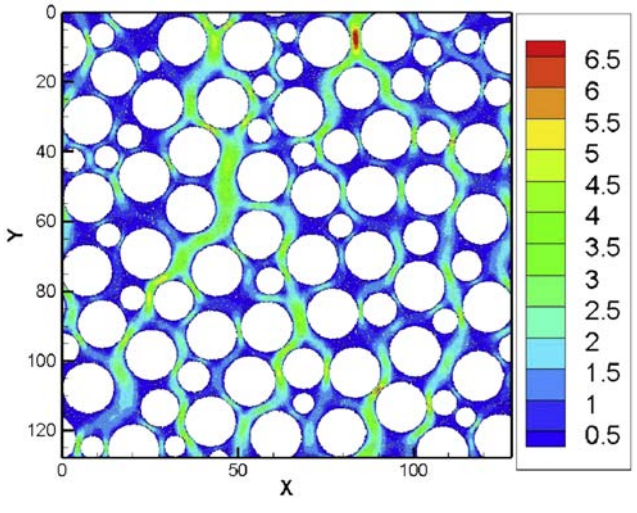


**Figure 10.** Heterogeneous pore-scale flow field showing the distribution of $v/\overline{v}$ (the magnitude of velocity relative to its spatial average), from *Tartakovsky and Neuman* [2008].

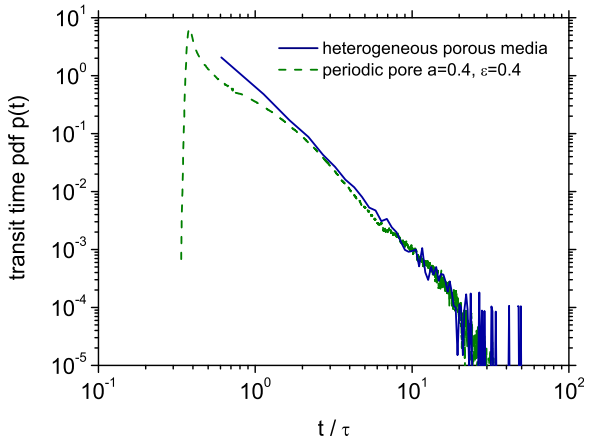


**Figure 11.** Transit time distribution across the mean pore size $\Delta x = 2.6$ for the heterogeneous porous media. It is compared here to the sinusoidal channel distribution for $a = 0.4$ and $\epsilon = 0.4$.

[29] The transit time distribution and transition matrix over the mean pore length $\Delta x = 2.6$ are computed by using $N = 27{,}620$ SPH particles (Figure 11). The comparison with the sinusoidal pore results shows that the large time distributions are strikingly similar for the two systems. The transition matrix (Figure 12) also shares some common features with those of the sinusoidal channel. The small transit times, corresponding to larger velocity channels, are found to be more correlated than other transit time classes. The large transit times are also more correlated than intermediate transit times, showing the existence of repetitive trapping phenomena. Thus, although the wavy channel model may appear simplified, it contains several features relevant to

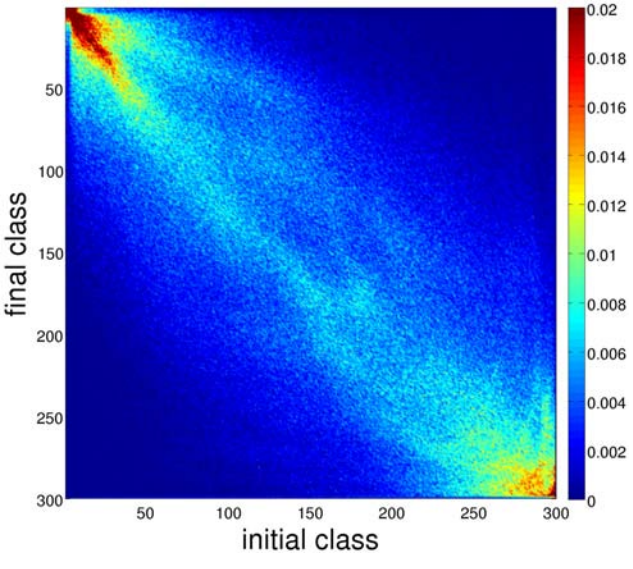


**Figure 12.** Spatial transition matrix $T$ across the mean pore size $\Delta x = 2.6$ for the heterogeneous porous medium. Small matrix indices correspond to small transit times (large Lagrangian velocities), and large matrix indices correspond to large transit times (small Lagrangian velocities). Here the matrix is discretized into 300 classes.

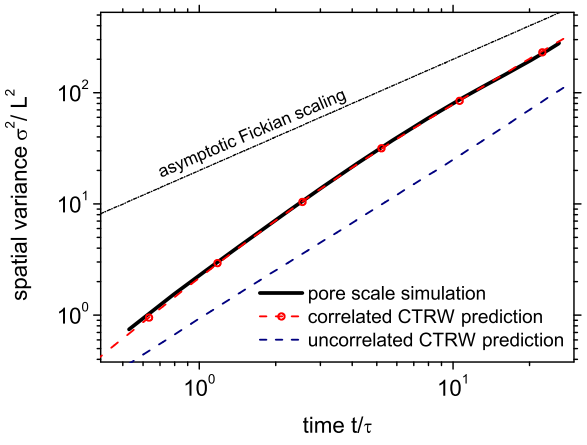


**Figure 13.** Comparison of the prediction of the correlated CTRW model (red dashed line) and the uncorrelated CTRW model (blue dashed line) for the second centered moment with the numerical simulations for the heterogeneous media (black line with dots). The variances are normalized by the mean pore size $L = 2.6$.

more complex media in regards to the transit time distribution and spatial correlation properties.

[30] The upscaled correlated CTRW model (equation (8)) can be parametrized by the transit time distribution $p(\Delta t)$ and the transition matrix **T**. As in the case of the sinusoidal channel model, the predictions for second centered moment $\sigma^2(t)$ compares well with the full numerical simulations at all times (Figure 13). Note that here the dispersion process is non-Fickian over the entire simulation time. It is expected to converge to Fickian at large time scales, when the particles have sampled the whole velocity distribution. The underestimation of dispersion by the uncorrelated CTRW model shows the importance of spatial correlations also in this system. This underlines the impact of incomplete mixing at pore throats on effective dispersion.

## 6. Conclusions

[31] The statistical analysis of pore-scale transit time series along particle trajectories (which can be thought of as the inverse of the Lagrangian velocities) shows that they can be represented as a spatial Markov process both for the wavy channel and heterogeneous porous media. The resulting upscaled CTRW model is shown to predict well the dispersion dynamics over the preasymptotic and asymptotic transport regimes.

[32] The correlated CTRW model that results from the spatial Markov property of the series of transition times contains complex correlation information. For instance, large velocities at the center of the pore are more correlated over successive pores than small velocities. The nontrivial dependence of dispersion on the pore boundary wall fluctuations can be quantified by the interplay and competition between distribution and correlation effects. In particular, successive trapping of particles in low-velocity and recirculation zones is found to be a key process. The two porous media studied here are two-dimensional. We expect that the transit time distribution and transition matrix would probably be quite different in the three-dimensional case. The spatial Markov property itself needs to be tested in this context.

[33] The upscaled correlated CTRW model is fully defined from the velocity distribution and spatial correlation properties. In this respect, the approach proposed here is different from that consisting in parametrizing an effective CTRW model from a breakthrough curve fit [e.g., *Berkowitz and Scher*, 2010]. In the latter approach, one can define an effective CTRW model with a limited number of parameters by not explicitly including spatial correlation effects. This approach is useful in field and experimental applications, for which one does not easily have access to the Lagrangian velocity field properties. For the porous media considered in this study, we show that establishing the relation between the upscaled CTRW model with the pore-scale velocity statistics requires to account explicitly for spatial correlation. The key physical process which is at the root of persistent correlation of Lagrangian velocities here is incomplete mixing at pore scale.

[34] **Acknowledgments.** We acknowledge the financial support of the French National Research Agency through the project MOHINI (ANR-07-VULN-008). The financial support of the European Commission through FP7 ITN IMVUL (grant agreement 212298) is gratefully acknowledged. T. Le Borgne acknowledges the support of the Marie Curie ERG grant Reactive-Flows (grant agreement 230947). D. Bolster would like to express thanks for financial support via NSF grant EAR-1113704. A. Tartakovsky was supported by the Advanced Scientific Computing Research Program of the Office of Science, U.S. Department of Energy, at the Pacific Northwest National Laboratory. The Pacific Northwest National Laboratory is operated for the U.S. Department of Energy by Battelle under contract DE-AC06-76RL01830. Any opinions, findings, conclusions, or recommendations do not necessarily reflect the views of the funding agencies.

## References

Aris, R. (1956), On the dispersion of solute in a fluid flowing through a tube, *Proc. R. Soc. London, Ser. A*, *235*, 67–77.

Attinger, S., I. Neuweiler, and W. Kinzelbach (2001), Macrodispersion in a radially diverging flow field with finite Peclet numbers: 2. Homogenization theory approach, *Water Resour. Res.*, *37*, 495–505.

Auriault, J., and P. Adler (1995), Taylor dispersion in porous media: Analysis by multiple scale expansions, *Adv. Water Resour.*, *18*, 217–226.

Bear, J. (1972), *Dynamics of Fluids in Porous Media*, Elsevier, New York.

Benson, D., S. Wheatcraft, and M. Meerschaert (2000), The fractional-order governing equation of Levy motion, *Water Resour. Res.*, *36*, 1413–1423.

Benson, D., R. Schumer, M. M. Meerschaert, and S. Wheatcraft (2001), Fractional dispersion, Levy motion, and the MADE tracer tests, *Transp. Porous Media*, *42*, 211–240.

Berkowitz, B., and H. Scher (1995), On characterization of anomalous dispersion in porous and fractured media, *Water Resour. Res.*, *31*, 1461–1466.

Berkowitz, B., and H. Scher (2010), Anomalous transport in correlated velocity fields, *Phys. Rev. E*, *81*, 011128, doi:10.1103/PhysRevE.81.011128.

Berkowitz, B., A. Cortis, M. Dentz, and H. Scher (2006), Modeling non-Fickian transport in geological formations as a continuous time random walk, *Rev. Geophys.*, *44*, RG2003, doi:10.1029/2005RG000178.

Bijeljic, B., and M. J. Blunt (2006), Pore-scale modeling and continuous time random walk analysis of dispersion in porous media, *Water Resour. Res.*, *42*, W01202, doi:10.1029/2005WR004578.

Bolster, D., T. Le Borgne, and M. Dentz (2009), Solute dispersion in channels with periodically varying apertures, *Phys. Fluids*, *21*, 056601.

Bouchaud, J. P., and A. Georges (1990), Anomalous diffusion in disordered media: Statistical mechanisms, models and physical applications, *Phys. Rep.*, *195*(4-5), 127–293.

Brenner, H. (1980), Dispersion resulting from flow through spatially periodic porous media, *Philos. Trans. R. Soc. London, Ser. A*, *297*, 81–133.

Brenner, H., and P. Adler (1982), Dispersion resulting from flow through spatially periodic porous media II. Surface and intraparticle transport, *Philos. Trans. R. Soc. London, Ser. A*, *307*, 149–200.

Carrera, J., X. Sanchez-Vila, I. Benet, A. Medina, G. Galarza, and J. Guimera (1998), On matrix diffusion: Formulations, solution methods and qualitative effects, *Hydrogeol. J.*, *6*, 178–190.

Chastanet, J., and B. D. Wood (2008), The mass transfer process in a two-region medium, *Water Resour. Res.*, *44*, W05413, doi:10.1029/2006WR005553.

Cherblanc, F., A. Ahmadi, and M. Quintard (2007), Two-domain description of solute transport in heterogeneous porous media: Comparison between theoretical predictions and numerical experiments, *Adv. Water Resour.*, *20*, 1127–1143.

Cushman, J., and T. Ginn (1993), Nonlocal dispersion in media with continuously evolving scales of heterogeneity, *Transp. Porous Media*, *13*, 123–138.

Cushman, J., and T. Ginn (1994), Nonequilibrium statistical mechanics of preasymptotic dispersion, *J. Stat. Phys.*, *75*, 859–878.

Cushman, J. H., and T. R. Ginn (2000), Fractional advection-dispersion equation: A classical mass balance with convolution-Fickian flux, *Water Resour. Res.*, *36*, 3763–3766.

Deng, F.-W., and J. Cushman (1995), Comparison of moments for classical-, quasi-, and convolution-Fickian dispersion of a conservative tracer, *Water Resour. Res.*, *31*, 1147–1149.

Deng, F.-W., J. H. Cushman, and J. W. Delleur (1993), A fast Fourier transform stochastic analysis of the contaminant transport process, *Water Resour. Res.*, *29*, 3241–3247.

Dentz, M., and D. Bolster (2011), Distribution- versus correlation-induced anomalous transport in quenched random velocity fields, *Phys. Rev. Lett.*, *105*, 244301.

Dentz, M., and A. Castro (2009), Effective transport dynamics in porous media with heterogeneous retardation properties, *Geophys. Res. Lett.*, *36*, L03403, doi:10.1029/2008GL036846.

Dentz, M., H. Kinzelbach, S. Attinger, and W. Kinzelbach (2000), Temporal behavior of a solute cloud in a heterogeneous porous medium: 1. Point-like injection, *Water Resour. Res.*, *36*, 3591–3604.

Dentz, M., D. Bolster, and T. Le Borgne (2009), Concentration statistics for transport in porous media, *Phys. Rev. E*, *80*, 010101.

Dentz, M., T. Le Borgne, A. Englert, and B. Bijeljic (2011), Mixing, spreading and reaction in heterogeneous media: A brief review, *J. Contam. Hydrol.*, *120–121*, 1–17.

Drazer, G., and J. Koplick (2002), Transport in rough self-affine fractures, *Phys. Rev. E*, *66*, 026303.

Drazer, G., H. Auradou, J. Koplik, and J. Hulin (2004), Self-affine front in self-affine fractures: Large and small-scale structure, *Phys. Rev. Lett.*, *92*, 014501.

Dykaar, B., and P. Kitanidis (1996), Macrotransport of a biologically reacting solute through porous media, *Water Resour. Res.*, *32*, 307–329.

Edwards, D., and H. Brenner (1993), *Macrotransport Processes*, Butterworth-Heinemann, Boston, Mass.

Edwards, D., M. Shapiro, H. Brenner, and M. Shapira (1991), Dispersion of inert solutes in spatially periodic, two-dimensional model porous media, *Transp. Porous Media*, *6*, 337–358.

Frankel, I., and H. Brenner (1989), On the foundations of generalized Taylor dispersion theory, *J. Fluid. Mech.*, *204*, 97–119.

Gelhar, L. (1993), *Stochastic Subsurface Hydrology*, Prentice Hall, Englewood Cliffs, N. J.

Gelhar, L., C. Welty, and K. Rehfeldt (1992), A critical review of data on field-scale dispersion in aquifers, *Water Resour. Res.*, *28*, 1955–1974.

Gill, W., and R. Sankarasubramanian (1970), Exact analysis of unsteady convective diffusion, *Proc. R. Soc. London, Ser. A*, *316*, 341–350.

Haggerty, R., and S. Gorelick (1995), Multiple-rate mass transfer for modeling diffusion and surface reactions in media with pore-scale heterogeneity, *Water Resour. Res.*, *31*, 2383–2400.

Kitanidis, P., and B. Dykaar (1997), Stokes flow in a slowly varying two-dimensional periodic pore, *Transp. Porous Media*, *26*, 89–98.

Latini, M., and A. Bernoff (2001), Transient anomalous diffusion in Poiseille flow, *J. Fluid. Mech.*, *441*, 399–411.

Le Borgne, T., and P. Gouze (2008), Non-Fickian dispersion in porous media: 2. Model validation from measurements at different scales, *Water Resour. Res.*, *44*, W06427, doi:10.1029/2007WR006279.

Le Borgne, T., J. de Dreuzy, P. Davy, and O. Bour (2007), Characterization of the velocity field organization in heterogeneous media by conditional correlation, *Water Resour. Res.*, *43*, W02419, doi:10.1029/2006WR004875.

Le Borgne, T., M. Dentz, and J. Carrera (2008a), Lagrangian statistical model for transport in highly heterogeneous velocity fields, *Phys. Rev. Lett.*, *101*, 090601, doi:10.1103/PhysRevLett.101.090601.

Le Borgne, T., M. Dentz, and J. Carrera (2008b), Spatial Markov processes for modeling Lagrangian particle dynamics in heterogeneous porous media, *Phys. Rev. E*, *78*, 026308, doi:10.1103/PhysRevE.78.026308.

Le Borgne, T., M. Dentz, P. Davy, D. Bolster, J. Carrera, J.-R. de Dreuzy, and O. Bour (2011), Persistence of incomplete mixing: A key to anomalous transport, *Phys. Rev. E*, *84*, 015301.

Levy, M., and B. Berkowitz (2003), Measurement and analysis of non-Fickian dispersion in heterogeneous porous media, *J. Contam. Hydrol.*, *23*, 2145–2154.

Lunati, I., S. Attinger, and W. Kinzelbach (2002), Macrodispersivity for transport in arbitrary nonuniform flow fields: Asymptotic and preasymptotic results, *Water Resour. Res.*, *38*(10), 1187, doi:10.1029/2001WR001203.

Matheron, G., and G. de Marsily (1980), Is transport in porous media always diffusive? A counterexample, *Water Resour. Res.*, *16*, 901–917.

Meyer, D. W., and H. Tchelepi (2010), Particle-based transport model with Markovian velocity processes for tracer dispersion in highly heterogeneous porous media, *Water Resour. Res.*, *46*, W11552, doi:10.1029/2009WR008925.

Morales-Casique, E., S. Neuman, and A. Guadagnini (2006), Nonlocal and localized analyses of nonreactive solute transport in bounded randomly heterogeneous porous media: Theoretical framework, *Adv. Water Resour.*, *29*, 1238–1255.

Moroni, M., N. Kelinfelter, and J. Cushman (2007), Analysis of dispersion in porous media via matched-index particle tracking velocimetry experiments, *Adv. Water Resour.*, *30*, 1–15.

Neuman, S. (1993), Eulerian-Lagrangian theory of transport in space-time nonstationary velocity fields: Exact nonlocal formalism by conditional moments and weak approximation, *Water Resour. Res.*, *29*, 633–645.

Neuman, S., and D. Tartakovsky (2009), Perspective on theories of anomalous transport in heterogeneous media, *Adv. Water Resour.*, *32*, 670–680.

Nicolaides, C., L. Cueto-Felgueroso, and R. Juanes (2010), Anomalous physical transport in complex networks, *Phys. Rev. E*, *82*, 055101.

Plumb, O., and S. Whitaker (1988), Dispersion in heterogeneous porous media: 1. Local volume averaging and large-scale averaging, *Water Resour. Res.*, *24*, 913–926.

Porter, M., F. Valdes-Parada, and B. Wood (2010), Comparison of theory and experiments for dispersion in homogeneous porous media, *Adv. Water Resour.*, *33*, 1043–1052.

Prude'Homme, R. K., and D. A. Hoagland (1999), Taylor-Aris dispersion arising from flow in a sinusoidal tube, *AIChE J.*, *31*, 236–244.

Rehfeldt, K., J. Boggs, and L. Gelhar (1992), Field study of dispersion in a heterogeneous aquifer: 3. Geostatistical analysis of hydraulic conductivity, *Water Resour. Res.*, *28*, 3309–3324.

Rosencrans, S. (1997), Taylor dispersion in curved channels, *SIAM J. Appl. Math.*, *57*, 1216–1241.

Sidle, R., B. Nilsson, M. Hansen, and J. Fredeicia (1998), Spatially varying hydraulic and solute transport characteristics of a fractured till determined by field tracer tests, Funen, Denmark, *Water Resour. Res.*, *24*, 2515–2527.

Silliman, S., and E. Simpson (1987), Laboratory evidence of the scale effect in dispersion of solutes in porous media, *Water Resour. Res.*, *23*, 1667–1673.

Silliman, S., L. Konikow, and C. Voss (1987), Laboratory experiment of longitudinal dispersion in anisotropic porous media, *Water Resour. Res.*, *23*, 2145–2154.

Tartakovsky, A., and S. Neuman (2008), Effects of Peclet number on pore-scale mixing and channeling of a tracer and on directional advective porosity, *Geophys. Res. Lett.*, *35*, L21401, doi:10.1029/2008GL035895.

Tartakovsky, D., and D. Xiu (2006), Stochastic analysis of transport in tubes with rough walls, *J. Comput. Phys.*, *217*, 248–259.

Tartakovsky, A. M., D. M. Tartakovsky, and P. Meakin (2008), Stochastic Langevin Model for Flow and Transport in Porous Media, *Phys. Rev. Lett.*, *101*, 044502, doi:10.1103/PhysRevLett.101.044502.

Taylor, G. (1953), Dispersion of soluble matter in solvent flowing slowly through a tube, *Proc. R. Soc. London, Ser. A*, *219*, 186–203.

Valdes-Parada, F., M. Porter, K. Narayanaswamy, R. Ford, and B. Wood (2009), Upscaling microbial chemotaxis in porous media, *Adv. Water Resour.*, *32*, 1413–1428.

Wood, B. (2009), The role of scaling laws in upscaling, *Adv. Water Resour.*, *32*, 723–736.

D. Bolster, Environmental Fluid Dynamics Laboratories, Department of Civil Engineering and Geological Sciences, University of Notre Dame, Notre Dame, IN 45665, USA.

P. de Anna and T. Le Borgne, Geosciences Rennes, UMR 6118, CNRS, Université de Rennes 1, F-35042 Rennes, France. (tanguy.le-borgne@univ-rennes1.fr)

M. Dentz, Institute of Environmental Assessment and Water Research, E-08034 Barcelona, Spain.

A. Tartakovsky, Computational Mathematics Group, Pacific Northwest National Laboratory, Richland, WA 99352, USA.